SUPPORTING INFORMATION

Supplementary Figure 1. Silencing of RIPK3, MLKL, and Bcl-x_L in Mφ infected with *Mtb* prevents necrosis. Human Mφ were transfected with RIPK3 (II) (A), MLKL siRNA (B) or scrambled control (Scr) RNA and gene expression was assessed using Western blotting. (A) RIPK3 (second siRNA) or (C) Bcl-x_L deficient **Mφ** were infected with H37Rv (MOI 5 or 10). Cell death was assessed using Live/Dead fixable dead cell stain kits (Invitrogen). Results are representative of pooling three wells per group and the numbers in histograms indicate the percentage of dead cells. Data are representative of 2-3 independent experiments. Results are represented as mean ± SE. Data were analyzed using one-way ANOVA. * Values of $P < 0.05$ were considered to be significant. Data are representative of 2 independent experiments.

Supplementary Figure 2. Avirulent *Mtb* induces apoptosis independent of RIPK3. BMD-Mφ from WT and RIPK3$^{-/-}$ mice were infected with H37Ra at MOI of ~10. After 12 h, expression of cleaved caspase 8 (A) and cleaved caspase 3 (B,C) was assessed using flow cytometry. (D) H37Ra infected WT and RIPK3$^{-/-}$Mφ were stained for Annexin V to assess apoptosis after 96h of infection. Results are represented as mean ± SE. Data were analyzed using one-way ANOVA. *,*** Values of $P < 0.05$, $P<0.01$, respectively were considered to be significant. Data are representative of 2 independent experiments.

Supplementary Figure 3. Silencing of the HKII or the RIPK3 genes suppresses NADH accumulation in Mφ infected with H37Rv. (**A**) Inputs for Figure 2 A. (**B**) Mφ transfected with HKII. RIPK3 siRNA or scrambled (Scr) control RNA (Scr) were infected with H37Rv (MOI 10). NADH levels were measured for HKII **(C)** and RIPK3 **(D)** silenced gene at 0, 6 and 24 h after infection (n=3).

Supplementary Figure 4. Gating strategy for assessing neutrophils in the lung. Lung cells were gated for leukocytes based on size (FSC-A) and granularity (SSC-A). Doublets were excluded by gating on FSC-A and FSC-H. Singlets were gated for viable cells. Prior to gate neutrophils, live cells were gated for CD11b+SSC-A+.

Supplementary Figure 5. RIPK3 deficient T cells have normal proliferative capacity *in vitro* and *in vivo*. (**A**) Splenic T cells were purified from naïve WT and RIPK3$^{-/-}$ mice using Pan T cell microbeads (MACS). T cells were then labeled with CFSE and cultured with or without anti-CD3 and anti-CD8 for 3 days. The percentage of T cell proliferation (CFSE dilution) was measured by FACS analysis. There was no difference between RIPK3$^{-/-}$ and WT CD3+CD4+ or CD3+CD8+ T cells proliferation. (**B** and **C**) Total cell number of CD4+ T cells and ESAT6-specific CD4+ T cells (**B**) as well as CD8+ T cells and TB10.4-specific CD8+ T cells (**C**) in lung at day 35 post-aersolized infection (H37Rv, 50-100 CFU). (**D**) ELISPOT of IFNγ production showing the frequency of *Mtb*-specific CD4^{+} and CD8^{+} T cells after 35 days of infection. Lung cells from infected RIPK3$^{-/-}$ and WT were cultured with ESAT6$_{(3-15)}$, Ag85B$_{(241-256)}$, TB10.4$_{(4-11)}$, and 32c$_{(309-318)}$. SFC, spot-forming cells. APC-conjugated streptavidin-phycoerythrin was used as a control for the tetramer staining. Five mice were individually analyzed and the data are given as mean value ± SE. (**E**) The number of bacteria in H37Rv-infected RIPK3$^{-/-}$ and WT Mφ prior to adoptive transfer.

Supplementary Figure 1

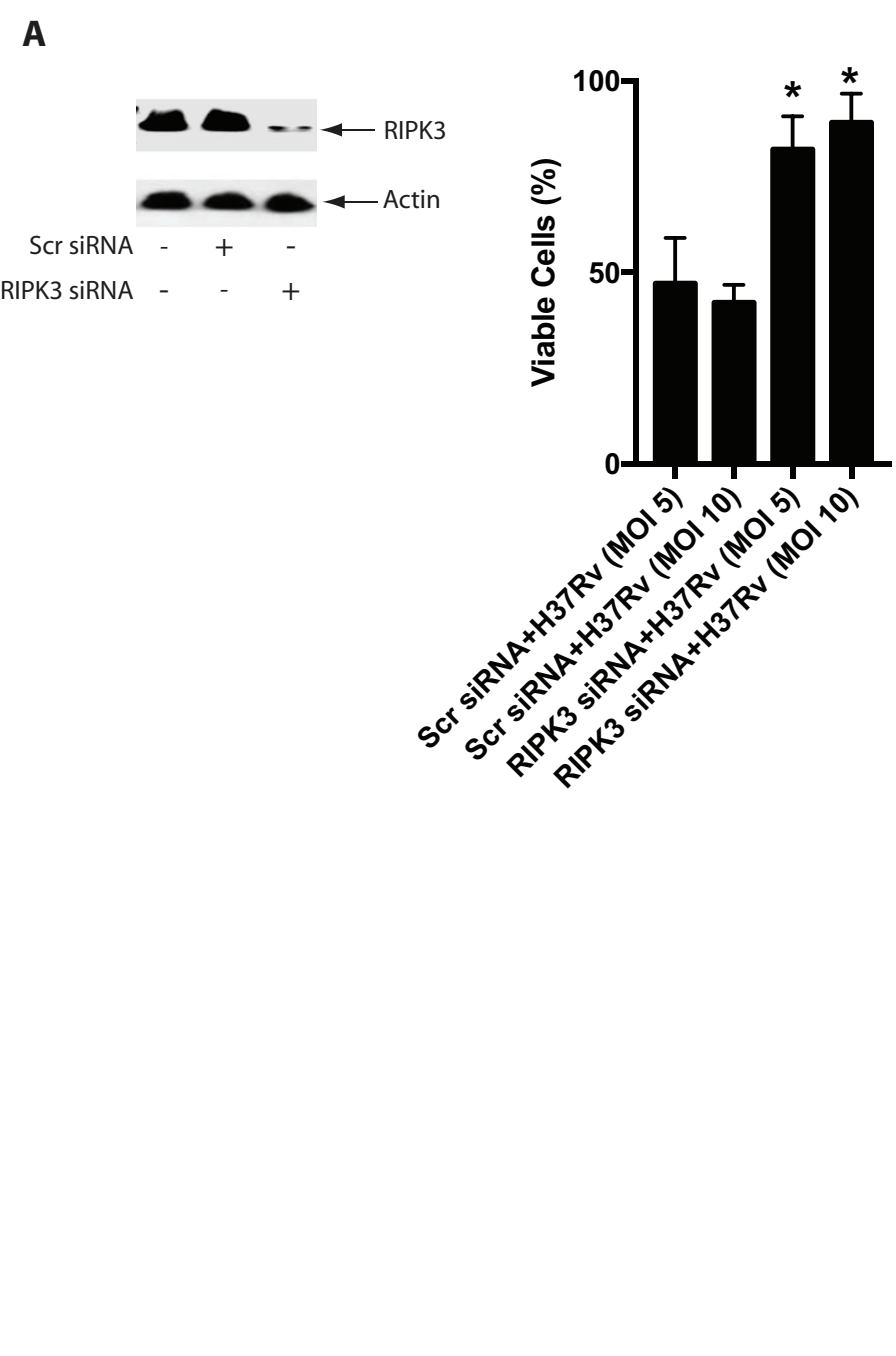

Supplementary Figure 2

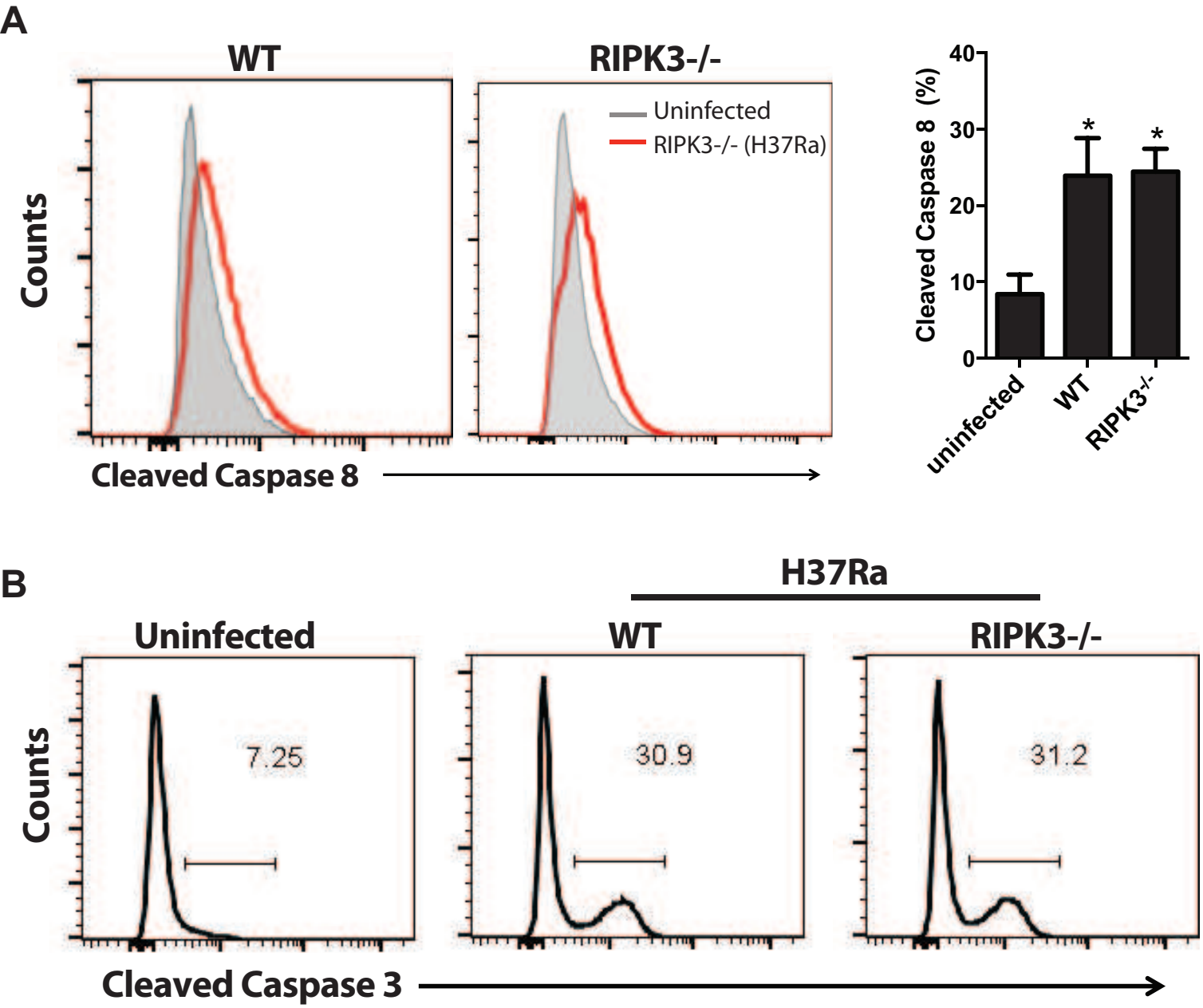

Supplementary Figure 3

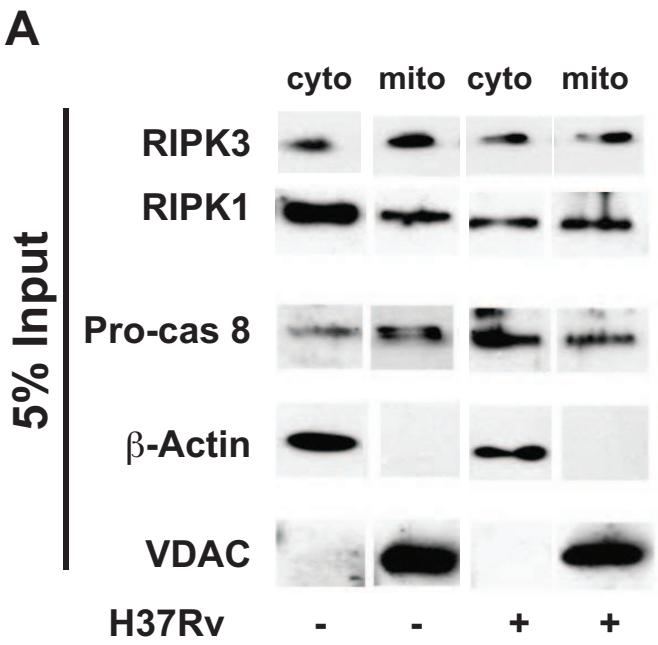

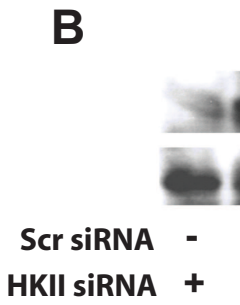

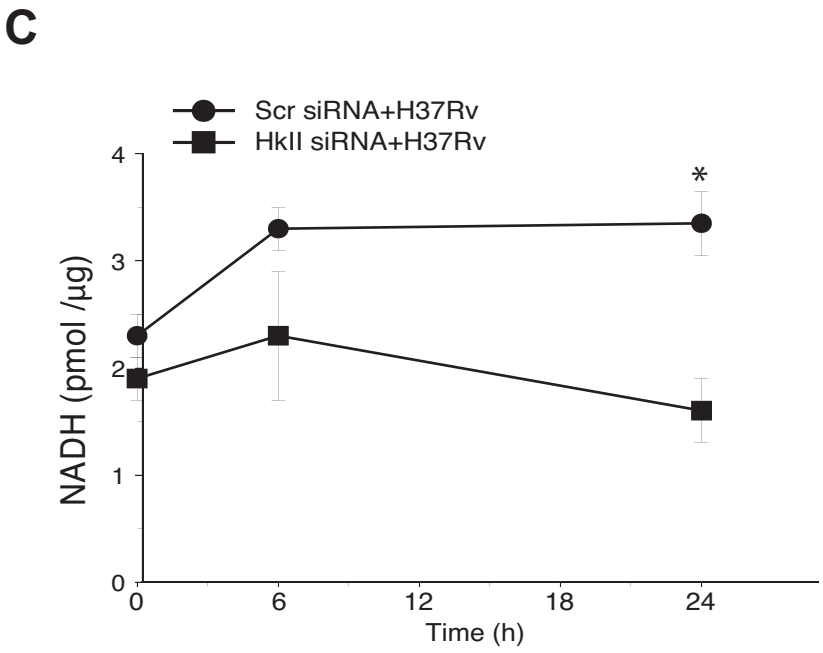

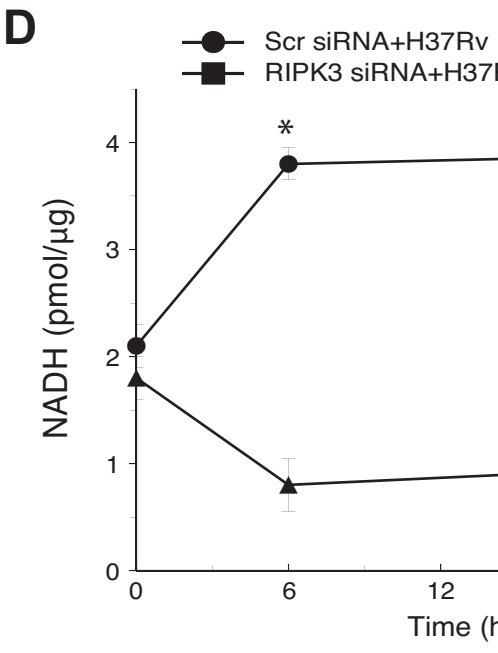

Supplementary Figure 4

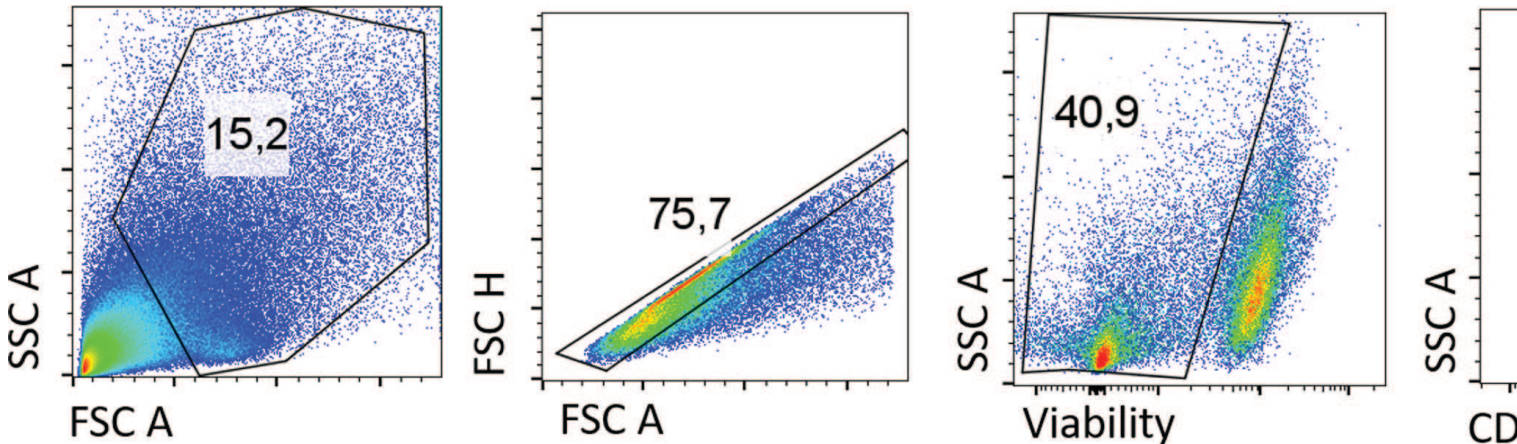

Supplementary Figure 5